

Spin structure factor and quantum phases of frustrated spin-1/2 chains

Manoranjan Kumar,¹ Aslam Parvej¹ and Z.G. Soos²

¹*S.N. Bose National Centre for Basic Sciences, Block-JD, Sector-III, Kolkata 700098, India.*

²*Department of Chemistry, Princeton University, Princeton, New Jersey 08544, USA.*

received and accepted dates provided by the publisher
other relevant dates provided by the publisher

PACS 75.10.Jm – Quantized spin model including frustrations
PACS 64.70.Tg – Quantum phase transition
PACS 73.22.Gk – Broken symmetry phases

Abstract – The static structure factor $S(q)$ of frustrated spin-1/2 chains with isotropic exchange and a singlet ground state (GS) diverges at wave vector q_m when the GS has quasi-long-range order (QLRO) with periodicity $2\pi/q_m$ but $S(q_m)$ is finite in bond-order-wave (BOW) phases with finite-range spin correlations. Exact diagonalization and density matrix renormalization group (DMRG) calculations of $S(q)$ indicate a decoupled phase with QLRO and $q_m = \pi/2$ in chains with large antiferromagnetic exchange between second neighbors. $S(q_m)$ identifies quantum phase transitions based on GS spin correlations.

Email: manoranjan.kumar@bose.res.in, soos@princeton.edu

1. Introduction

The J_1J_2 model with isotropic exchange $J_1, J_2 > 0$ between first and second neighbors is the prototypical frustrated spin-1/2 chain with a bond-order-wave (BOW) phase.¹⁻¹⁵ The Hamiltonian with periodic boundary conditions (PBC) and frustration $g = J_2/J_1 > 0$ is

$$H(g) = \sum_p (\vec{s}_p \cdot \vec{s}_{p+1} + g \vec{s}_p \cdot \vec{s}_{p+2})$$

$$= g(H_A + H_B) + \sum_p \vec{s}_p \cdot \vec{s}_{p+1} \quad (1)$$

H_A and H_B are linear Heisenberg antiferromagnets (HAFs) with PBC on sublattices of odd and even-numbered sites, and $H(0)$ is also an HAF. The ground state (GS) of Eq. 1 is a singlet, $S=0$. The infinite chain has nondegenerate GS at small g that becomes doubly degenerate⁸ at $g^* = 0.2411$, the boundary of the BOW phase with broken inversion symmetry at sites and a finite energy gap² $E_m(g)$ to the lowest triplet state. The exact GS at the Majumdar-Ghosh point,¹ $g = 1/2$, are the Kekulé diagrams $|K1\rangle$ and $|K2\rangle$ of organic chemistry that correspond to singlet-paired spins on adjacent sites. Recent studies¹⁶⁻²⁰ have focused on ferromagnetic $J_1 < 0$ as the starting point for modeling oxides with chains of $s = 1/2$ Cu(II) ions.

Bursill et al.¹⁰ studied the static spin structure factor $S(q;g)$ of the J_1J_2 model and took the $S(q_m)$ peak as the effective periodicity $2\pi/q_m$. They compared q_m to

chains of classical spins, for which the GS energy of Eq. 1 goes as $\cos\chi + g\cos 2\chi$ where χ is the pitch angle between successive spins. Minimization gives $\cos\chi = -1/4g$, or $\chi = \pi$ for $g < 1/4$ and a continuous decrease to $\chi = \pi/2$ as $g \rightarrow \infty$. Quantum effects¹⁰ are pronounced at small g , where $q_m = \pi$ persists to $g = 1/2$. The BOW phase extends to arbitrarily large g according to Bursill et al.¹⁰ and the field theories of White and Affleck¹¹ and Itoi and Qin¹³. We find instead that the BOW phase terminates at $1/g^{**} \sim 0.40$ at the start of a gapless decoupled phase^{21,22} with nondegenerate GS. We return in the Discussion to reasons for reexamining the quantum phase diagram at large g .

In this paper, the *magnitude* of $S(q_m;g)$ is applied to the quantum phase diagram of frustrated spin chains. $S(q_m;g)$ diverges when the GS has quasi-long-range order (QLRO) at wave vector q_m . The HAF at $g = 0$ has QLRO(π) while the BOW phase has finite $S(q_m;g)$ and spin correlations that are just to nearest neighbors at $g = 1/2$. The quantum transition between the QLRO(π) and BOW phases is the largest g at which $S(\pi;g)$ diverges; as shown in Section 3, this agrees with $g^* = 0.2411$ based⁸ on the degeneracy, $E_m = E_\sigma$, of the triplet and lowest singlet excitation. HAFs on sublattices at $1/g = 0$ have QLRO($\pi/2$) and divergent $S(\pi/2;\infty)$. The largest $1/g$ at which $S(\pi/2;g)$ diverges marks the transition from the decoupled to the BOW phase. In our analysis, the frustrated BOW phase with finite $S(q;g)$ is intermediate between phases with dominant QLRO(π) at small g and QLRO($\pi/2$) at small $1/g$.

We obtain $S(q;g)$ using exact diagonalization (ED) of finite J_1J_2 models, density matrix

renormalization group (DMRG) calculations and extrapolation to the infinite chain. The procedure is general for spin chains. Sections 2 and 3 present $S(q;g)$ results and the size dependence of $S(q_m;g)$, respectively. In Section 4 we briefly discuss the gapless decoupled phase and specific challenges of solving $H(g)$ at large g .

2. Static structure factor $S(q)$

The static structure factor $S(q)$ of 1D systems with one spin per unit cell is the GS expectation value

$$\begin{aligned} S(q) &= \frac{1}{N} \sum_{p,r} \langle \vec{s}_p \cdot \vec{s}_r \rangle e^{iq(p-r)} \\ &= \sum_p \langle \vec{s}_1 \cdot \vec{s}_{1+p} \rangle e^{iqp} \end{aligned} \quad (2)$$

The wave vectors in the first Brillouin zone are $q = 2\pi m/N$ with $m = 0, \pm 1, \dots, N/2$. We define spin correlation functions $C(p;g) = \langle \vec{s}_1 \cdot \vec{s}_{1+p} \rangle$ at frustration g in Eq. 1 and consider $S(q;g,4n)$ with $N = 4n$ spins that ensure integer total spin $S \leq 2n$ and sublattice spin $S_A, S_B \leq n$. The $q = 0$ component satisfies $S(0;g) = \langle S^2 \rangle / 4n = 0$ when the GS is a singlet; the sum of $C(p;g)$ over p is zero; summing over q in the Brillouin zone and taking the limit $n \rightarrow \infty$ leads to

$$\begin{aligned} \frac{1}{4n} \sum_q S(q;g,4n) &= \frac{3}{4} \\ &= \frac{1}{\pi} \int_0^\pi dq S(q;g) \end{aligned} \quad (3)$$

since $C(0,g) = 3/4$ for $s = 1/2$.

If the $C(p;g)$ have finite range, $S(q;g)$ is finite and the sum in Eq. 2 becomes constant once the system size exceeds the correlation length. For even N in Eq. 2, the exact GS at $g = 1/2$ gives

$$S(q;1/2) = 3(1 - \cos q) / 4 \quad (4)$$

The size dependence is entirely in the discrete q values. A finite energy gap $E_m(g)$ in the BOW phase indicates a localized GS and finite-range spin correlations. $S(q;g)$ is readily found directly for some g in the BOW phase. We defer to Section 3 the numerical problem of the divergence of $S(q_m;g)$.

To illustrate, we choose g in Eq. 1 such that 24 spins is close to the infinite chain. The peak is better seen in the zone $0 \leq q < 2\pi$. Open symbols in the upper panel of Fig. 1 are exact $S(q;g,24)$ at discrete q in Eq. 2 for $g = 0.40, 0.50, 0.70$ and 1.0 . Solid lines are

$S(q;g,48)$ with continuous q obtained by DMRG for 48 spins. Almost identical $S(q;g)$ are found except at $g = 1$

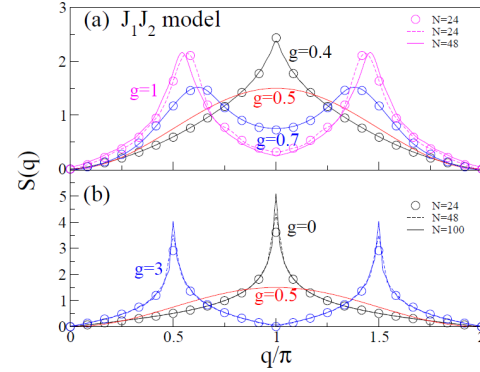


Fig. 1. Spin structure factor $S(q)$, Eq. 2, with frustration g in the J_1J_2 model, Eq. 1. Open symbols are exact for $N = 24$ spins and discrete wave vectors q . (a) $S(q)$ is finite in the BOW phase. Solid lines are DMRG results for $N = 48$ spins and continuous q ; the dashed line at $g = 1$ has 24 spins and continuous q . (b) Solid lines and dashed lines are DMRG results for $N = 100$ and 48 spins. The $S(q)$ peaks at $q = \pi$ for $g = 0$ and at $\pm\pi/2$ for $g = 3$ increases with system size in phases with quasi-long-range order.

where the dashed line refers to 24 spins and continuous q . The peak at $q_m = \pi$ for $g = 0.40$ and 0.50 evolves with increasing g to $\pi/2$ and $3\pi/2$ ($-\pi/2$).

The HAF is a gapless spin liquid²³ with $QLRO(\pi)$, algebraically decreasing $C(p,0)$ and divergent $S(\pi;0)$. At $1/g = 0$, we have HAFs on sublattices, $QLRO(\pi/2)$ and divergent $S(\pi/2;\infty)$. The lower panel of Fig. 1 contrasts $S(q;g)$ at $g = 0$ and 3 with $g = 1/2$. Open symbols are exact $S(q;g,24)$ at $g = 0$ and 3 ; the dashed and solid lines are DMRG results for 48 and 100 spins, respectively. Quite generally, we have $S(q;0,4n) = S(q/2;\infty,8n)$ since both $g = 0$ and $1/g = 0$ correspond to $4n$ -spin HAFs. The $q_m = \pi$ peak for 24 spins at $g = 0$ is almost exactly equal to the $q_m = \pi/2$ peak for 48 spins at $g = 3$. Fig. 1 already suggests that the BOW phase does not extend to $g = 3$. As shown in Section 3, the lowest-order changes go as

$$\begin{aligned} S(\pi;g,4n) &= S(\pi;0,4n) - A_n g \\ S(\pi/2;1/g,8n) &= S(\pi/2;0,8n) - B_n / g^2 \end{aligned} \quad (5)$$

with $A_n, B_n > 0$. Since the peaks are equal at $g = 0 = 1/g$, the $\pi/2$ peak in finite systems is less sensitive to frustration $1/g \ll 1$ than the π peak is to $g \ll 1$.

The wave vector q_m is shown in Fig. 2 as a function of $g/(1+g)$. Open circles are exact for 24 spins. The peak remains at π up to $g = 1/2$ and then decreases to

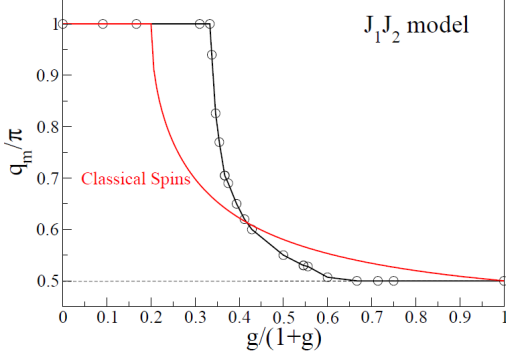


Fig. 2. Wave vector q_m of the structure factor peak $S(q_m)$ of the J_1J_2 model with $N = 24$ spins as function of frustration $g/(1+g)$. The chain of classical spins has pitch angle $\chi = \pi$ for $g \leq 1/4$ and $\chi = \cos^{-1}(-1/4g)$ for $g > 1/4$.

$q_m = \pi/2$. Classical spins have pitch angle q_m , with $\cos q_m = -1/4g$ for $g > 1/4$, doubly degenerate GS with long-range Néel order up to $g = 1/4$, and a spiral GS with LRO(q_m) for $g > 1/4$. We find strong quantum effects at large g that compress the BOW phase and lock in $q_m = \pi/2$.

3. Phase transitions

The static structure factor identifies the three quantum phases of the J_1J_2 model. The location of phase transitions is more demanding. Finite N in Eq. 2 clearly gives finite $S(q)$. We must infer whether $S(\pi;g,4n)$ or $S(\pi/2;g,4n)$ diverges with increasing system size rather than merely becoming large. The numerical problem is to compute all spin correlations $C(p,g)$ in systems of $N = 4n$ spins. We use ED up to 24 spins and a finite DMRG algorithm for larger systems with four spins added per step¹⁵ and cyclic boundary conditions.²⁴ The algorithm is more accurate than conventional DMRG because adding four spins per step ensures that the sublattices always have $S_A = S_B = 0$ at $1/g = 0$ rather than $S_A = S_B = 1/2$ at every other step. Truncation errors in the sum of the eigenvalues of the density matrix are less than 10^{-10} in the worst case when $m = 200$ eigenvalues are kept. Finite size effects increase at large g . DMRG returns $C(p,g)$ whose accuracy can be tested rigorously by comparison to the exact result, $S(0;g,4n) = 0$. We find $S(0;g,100) < 10^{-3}$ in the QLRO(π) phase up to $4n = 100$ and comparable accuracy to $4n = 64$ in the QLRO($\pi/2$) phase.

We also rely on HAF spin correlation functions²³ that establish the divergence of $S(\pi;0)$ or $S(\pi/2;\infty)$. The $q = \pi$ term of Eq. 2 for $4n$ spins is

$$S(\pi;g,4n) = \frac{3}{4} + C(2n,g) + 2 \sum_{p=1}^{2n-1} C(p,g)(-1)^p \quad (6)$$

Since $C(p,0)$ goes as $(-1)^p$, the sum is over $|C(p,0)|$. As shown in the inset to Fig. 3, $S(\pi;g,4n)$ is a linear function at small g with slope $-A_n$ and $A_6 = 1.6$ for 24 spins. Finite $g > 0$ is frustrating while $g < 0$ enhances short-range $q = \pi$ order.

Incremental increases of $S(\pi;g,4n)$ from $4n$ to $4n + 4$ spins are shown in Fig. 3 as a function of $100/N$ with $N = 4n + 2$, followed by linear extrapolation to the infinite chain. $S(\pi;0.40,4n)$ converges rapidly as noted in Fig. 1. Within our accuracy, $S(\pi;g)$ diverges at $g = 0.20$ and converges at $g = 0.25$. The estimated g^* between 0.20 and 0.25 based on the structure factor is consistent with, but much less precise than $g^* = 0.2411$ based⁸ on $E_m = E_\sigma$. The two methods are independent since the GS determines $S(\pi;g)$ but does not enter in the excited-state degeneracy.

Only spin correlations within one sublattice contribute to $S(\pi/2)$

$$S(\pi/2;g,4n) = \frac{3}{4} + C(2n,g)(-1)^n + 2 \sum_{p=1}^{n-1} C(p,g) \cos(\pi p/2) \quad (7)$$

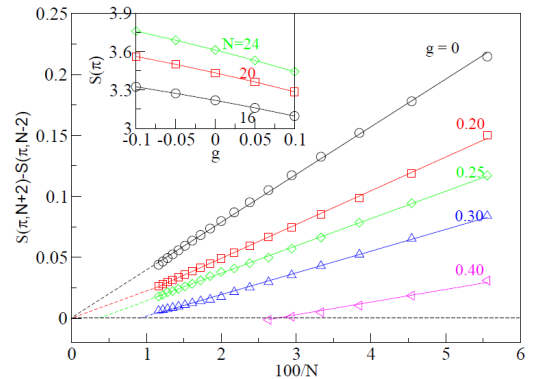


Fig. 3. Incremental increase of the structure factor peak $S(\pi,4n)$ from n to $n + 1$ as a function of $1/N$ with $N = 4n + 2$ using ED up to 24 spins, DMRG to 100 spins and linear extrapolation to the infinite chain; $S(\pi;g)$ diverges at $g = 0.20$, converges at $g = 0.25$. Inset: linear dependence of $S(\pi;g)$ on g near the origin for 16, 20 and 24 spins.

The $\pi/2$ peak for $8n$ spins reduces as expected to Eq. 6. In contrast to $S(\pi, g)$ at small g , however, there is no linear contribution in $1/g$ because $J_2 > 0$ is frustrating for either sign of J_1 . The first-order correction $|\phi\rangle$ in $1/g$ is given by

$$(H_A + H_B - 2E_0)|\phi\rangle = -\frac{1}{g} \sum_p \bar{s}_p \cdot \bar{s}_{p+1} |G_A\rangle |G_B\rangle \quad (8)$$

H_A and H_B are HAFs on sublattices whose singlet GS and energy are $|G\rangle$ and E_0 . Adjacent spins generate a singlet linear combination of triplets on each sublattice; $|\phi\rangle$ is a linear combination of such product states. Without explicitly solving Eq. 8, we obtain the general result for N

$$\langle \phi | \bar{s}_1 \cdot \bar{s}_{1+2p} | G_A \rangle | G_B \rangle = 0 \quad (9)$$

When both spins are in the same sublattice, the matrix element is zero since the triplet and GS of the other sublattice are orthogonal. It follows that $C(2p, g)$ and hence $S(\pi/2; g, 8n)$ initially decreases as $1/g^2$.

Figure 4 shows incremental increases of $S(\pi/2; g, 8n)$ from $8n$ to $8n + 8$ spins as a function of $100/N$ with $N = 8n + 4$, followed by linear extrapolation to the infinite chain. The $1/g = 0$ points to 200 spins are $g = 0$ results to 100 spins. As noted above, shorter chains of 64 spins meet the requirement of $S(0; g) < 10^{-3}$ at large g . $S(\pi/2, g)$ converges and is clearly finite at $g = 2.0$ in the BOW phase. The estimated transition g^{**} between the BOW and decoupled phases is around $1/g^{**} \sim 0.40$. As shown in the inset, $S(\pi/2; g, 8n)$ initially goes as $-B_n/g^2$ with $B_6 = 0.17$ for 24 spins and is almost constant.

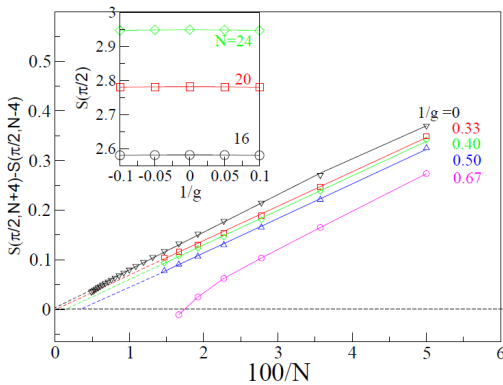


Fig. 4. Incremental increase of the structure factor peak $S(\pi/2, 8n)$ from n to $n + 1$ as a function of $1/N$ with $N = 4n + 4$ using ED up to 24 spins, DMRG to 64 spins and linear extrapolation to the infinite chain; $S(\pi/2, g)$ diverges at $1/g = 0.33$, converges at $1/g = 0.50$. Inset:

quadratic dependence of $S(\pi/2; g)$ on $1/g$ near the origin for 16, 20 and 24 spins; the maxima are at $1/g = 0$.

To summarize the $S(q_m; g)$ results, we return to Eq. 5. The divergences at $g = 0$ and $1/g = 0$ are identical. Since finite systems to 24 spins have $A_n > B_n$ by an order of magnitude, initial deviations $-B_n/g^2$ from $1/g = 0$ are much smaller than $-A_n g$ from $g = 0$. The BOW transition g^* based on the divergence of $S(\pi; g)$ in Fig. 3 is consistent with $g^* = 0.2411$ based on $E_m = E_\sigma$. The transition at $1/g^{**} \sim 0.40$ from the BOW to decoupled phase in Fig. 4 is consistent with $g^{**} = 2.1$ based¹⁴ on the $E_m = E_\sigma$ at large g . The $1/g^2$ decrease in Eq. 5 extends the decoupled phase to $J_1 < 0$.

4. Discussion

We have related the structure factor peak, $S(q_m; g)$, to the quantum phases of the $J_1 J_2$ model, Eq. 1. $S(q_m; g)$ diverges at $q_m = \pi$ up to g^* in the spin liquid phase with QLRO(π), is finite in the frustrated BOW phase between g^* and g^{**} , and diverges for $g > g^{**}$ in the gapless decoupled phase with QLRO($\pi/2$). We now address conflicting results that extend the BOW phase to $1/g = 0$.

To start with, theoretical and numerical works¹⁻¹³ have focused mainly on the quantum phase transition at g^* to the BOW phase and recent studies¹⁶⁻²⁰ of Eq. 1 also deal with other sectors than large g . Interesting and exotic GS are generated by an external magnetic field, by anisotropic or antisymmetric rather than isotropic exchange, by changing the sign of J_1 or by increasing the range of exchange interactions. The magnetic properties of organic and inorganic crystals that contain spin chains provide other applications.

There are several reasons for a closer look at the $1/g \ll 1$ regime. First, the initial DMRG calculations¹¹ were limited to $1/g > 0.5$, far from the limit. Second, Okamoto and Namura⁸ used ED in finite systems to obtain g^* from the degeneracy $E_m = E_\sigma$; the same degeneracy at $1/g^{**}$ was not pointed out until later.¹⁴ As a matter of consistency, ED in finite systems cannot decide for locating the phase transition at g^* but irrelevant at g^{**} . Third, exact HAF states describe both limits. ED of Eq. 1 with $4n$ spins yields n points g_n with doubly degenerate GS and broken inversion symmetry, starting with $g_1 = 1/2$. The degenerate GS at the largest g_n are closely related²¹ to the product of sublattice ground states, $|G_A\rangle |G_B\rangle$, and the singlet linear combination of the lowest triplets, $^1|T_A\rangle |T_B\rangle$. In view of the insets to Figs. 3 and 4, it would be remarkable have a nondegenerate GS with divergent $S(\pi; g)$ up to g^* while strictly limiting nondegenerate GS and divergent $S(\pi/2; g)$ to $1/g = 0$.

The large- g sector of Eq. 1 is particularly challenging, a point that may be relevant to spin chains as many-body problems. Field theories^{11,13} starting with an HAF at $g = 0$ lead to different expressions for E_m and rely on the same limited¹¹ DMRG for numerical support. Allen and Senechal¹² start with two HAFs at $1/g = 0$ and discuss three different continuum descriptions of Eq. 1 along with various approximations. Turning to DMRG, we note that open boundary conditions (OBC) are typically used for an even number of spins. Quite aside from strong end effects,¹⁵ inversion symmetry at sites is lost for even N . We find doubly degenerate GS and broken inversion symmetry at sites for $N = 4n$ spins and PBC in Eq. 1 at n values of g . OBC not only lifts the degeneracy²¹ but reverses the order to $E_m < E_\sigma$. Finally, accurate Monte Carlo methods have recently been devised²³ for 1D spin systems, including HAFs, but not for frustrated models due to a sign problem. Large g presents open questions for both field theory and numerical methods.

The magnitude of $S(q_m;g)$ bears directly on the quantum phases of frustrated spin chains. ED partly compensates for finite-size limitations by returning exact correlation functions $C(p,g)$. $S(q;g)$ is found directly for short-range correlation. Extrapolation to infinite chains is guided by the known HAF divergences of $S(\pi;0)$ or $S(\pi/2;\infty)$. But extrapolation entails approximations. Numerical methods and field theory are in agreement for the quantum transition of the J_1J_2 model from the QLRO(π) to BOW phase at $g^* = 0.2411$, but disagree at present at large g . The peak $S(q_m;g)$ is finite in the BOW phase, diverges at $q_m = \pi$ for $g < g^*$ in the spin liquid phase with QLRO(π) and at $q_m = \pi/2$ for $1/g > 1/g^{**}$ in the decoupled phase. Frustrated spin chains whose GS has LRO(π) at $g = 0$ undergo a first order quantum transition²¹ with increasing g directly to the decoupled phase. The transition occurs at $g_c = 1/4\ln 2$ in an analytical model²¹ with equal $J = 2/(4n - 1)$ between spins in opposite sublattices and $-J$ between spins in the same sublattice.

Acknowledgments: We thank D. Sen, A.W. Sandvik and S. Ramasesha for instructive discussions of BOW phase systems and the NSF for partial support of this work through the Princeton MRSEC (DMR-0819860). MK thanks DST for a Ramanujan Fellowship and support for thematic unit of excellence on computational material science.

References

1. C.K. Majumdar and D.K. Ghosh, *J. Math. Phys.* **10**, 1399 (1969).

2. B.S. Shastri and B. Sutherland, *Phys. Rev. Lett.* **47**, 964 (1981).
3. F.D.M. Haldane, *Phys. Rev. B* **25**, 4925 (1982).
4. K. Kuboki and H. Fukuyama, *J. Phys. Soc. Japan* **56**, 3126 (1987).
5. T. Tonegawa and I. Harada, *J. Phys. Soc. Japan* **56**, 2153 (1987).
6. I. Affleck, T. Kennedy, E.H. Lieb and H. Tasaki, *Commun. Math. Phys.* **115**, 477 (1988).
7. I. Affleck, D. Gepner, H.J. Schultz and T. Ziman, *J. Phys. A* **22**, 511 (1989).
8. K. Okamoto and K. Namura, *Phys. Lett. A* **169**, 433 (1992).
9. R. Chitra, S. K. Pati, H. R. Krishnamurthy, D. Sen and S. Ramasesha, *Phys. Rev. B* **52**, 6581 (1995).
10. R. Bursill, G.A. Gehring, D.J.J. Farnell, J.B. Parkinson, T. Xiang and C/ Zeng, *J. Phys: Condens. Matter* **7**, 8605 (1995).
11. S.R. White and I. Affleck, *Phys. Rev. B* **54**, 9862 (1996).
12. D. Allen and D. Senechal, *Phys. Rev. B* **55**, 299 (1997).
13. C. Itoi and S. Qin, *Phys. Rev. B* **63**, 224423 (2001).
14. M. Kumar, S. Ramasesha and Z.G. Soos, *Phys. Rev. B* **81**, 054413 (2010).
15. M. Kumar, Z. G. Soos, D. Sen, and S. Ramasesha, *Phys. Rev. B* **81**, 104406 (2010).
16. S. Furukawa, M. Sato and S. Onoda, *Phys. Rev. Lett.* **105**, 257205 (2010).
17. D.V. Dmitriev and V. Ya. Krivnov, *Phys. Rev. B* **77**, 024401 (2008).
18. T. Hikihara, L. Kecke, T. Momoi, and A. Furusaki, *Phys. Rev. B* **78**, 144404 (2008).
19. J. Sirker, V.Y. Krivnov, D.V. Dmitriev, A. Herzog, O. Janson, S. Nishimoto, S.-L. Drechsler, and J. Richter, *Phys. Rev. B* **84**, 144403 (2011).
20. M. Kumar and Z.G. Soos, *Phys. Rev. B* **85**, 144415 (2012).
21. M. Kumar and Z.G. Soos, *Phys. Rev. B* **88**, 134412 (2013).
22. M. Kumar, S. Ramasesha and Z.G. Soos, *Croatia Chem. Acta* **86**, 407 (2013).
23. A. W. Sandvik, *AIP Conf. Proc.* **1297**, 135 (2010) and references therein.
24. M. Kumar, S. Ramasesha and Z.G. Soos, *Phys. Rev. B* **79**, 035102 (2009).